Pak1 regulates focal adhesion strength, myosin IIA distribution, and actin dynamics to optimize cell migration

Violaine D. Delorme-Walker,[1,2] Jeffrey R. Peterson,[3] Jonathan Chernoff,[3] Clare M. Waterman,[4] Gaudenz Danuser,[5] Céline DerMardirossian,[1,2] and Gary M. Bokoch[1,2]

[1]Department of Immunology and Microbial Sciences and [2]Department of Cell Biology, The Scripps Research Institute, La Jolla, CA 92037
[3]Basic Sciences Division, Fox Chase Cancer Center, Philadelphia, PA 19111
[4]Cell Biology and Physiology Center, National Heart, Lung, and Blood Institute, National Institutes of Health, Bethesda, MD 20892
[5]Department of Cell Biology, Harvard Medical School, Boston, MA 02115

Cell motility requires the spatial and temporal coordination of forces in the actomyosin cytoskeleton with extracellular adhesion. The biochemical mechanism that coordinates filamentous actin (F-actin) assembly, myosin contractility, adhesion dynamics, and motility to maintain the balance between adhesion and contraction remains unknown. In this paper, we show that p21-activated kinases (Paks), downstream effectors of the small guanosine triphosphatases Rac and Cdc42, biochemically couple leading-edge actin dynamics to focal adhesion (FA) dynamics. Quantitative live cell microscopy assays revealed that the inhibition of Paks abolished F-actin flow in the lamella, displaced myosin IIA from the cell edge, and decreased FA turnover. We show that, by controlling the dynamics of these three systems, Paks regulate the protrusive activity and migration of epithelial cells. Furthermore, we found that expressing Pak1 was sufficient to overcome the inhibitory effects of excess adhesion strength on cell motility. These findings establish Paks as critical molecules coordinating cytoskeletal systems for efficient cell migration.

Introduction

Cell migration is central to many biological and pathological processes including, but not limited to, embryogenesis, tissue repair, immune response, atherosclerosis, and cancer. Crawling motility involves a four-step cycle. Polymerization of the lamellipodial actin cytoskeletal network drives the initial extension of the plasma membrane at the cell front (Pollard and Borisy, 2003). Cells then form adhesions to the ECM by recruiting signaling and cytoskeletal proteins to stabilize the protrusion at the lamellipodium base (Ridley et al., 2003). The contractile F-actin–myosin network located in the lamella and the ventral cell area uses these adhesions as sites to pull the cell body forward. Adhesion disassembly occurs both at the cell front and at the cell rear. In the front of migrating cells, the continuous formation and disassembly of adhesions, referred to as adhesion turnover, is highly regulated and is coupled to protrusion formation (Webb et al., 2004). Release of the adhesions and retraction at the rear completes the migratory cycle, allowing net translocation of the cell in the direction of the movement (Le Clainche and Carlier, 2008).

Although it has long been known that the ability of cells to move effectively depends on an optimum level of ECM for adhesion, recent data indicate that such optimized cell migration results from the interdependent feedback between F-actin polymerization/depolymerization and motility-activated myosin II and focal adhesion (FA) assembly/disassembly (Gupton and Waterman-Storer, 2006). Missing from this important study was any indication of the specific biochemical pathways that enabled upstream signals originating from RhoGTPases to regulate this complex interplay between integrins and the cytoskeleton.

C. DerMardirossian and G.M. Bokoch contributed equally to this paper.

Dr. Bokoch died on 10 January 2010.

Correspondence to Céline DerMardirossian: dmceline@scripps.edu

Abbreviations used in this paper: CB, cytoskeletal buffer; FA, focal adhesion; FN, fibronectin; FSM, fluorescent speckle microscopy; MHC, myosin IIA heavy chain; MLC, myosin light chain; Pak, p21-activated kinase; PID, Pak autoinhibitory domain; PIR, Pak inhibitor related; pMLC, phosphorylated myosin II regulatory light chain; pPak, phosphorylated Pak; qFSM, quantitative FSM; TIRF, total internal reflection fluorescence; WT, wild type.

The Rockefeller University Press $30.00
J. Cell Biol. Vol. 193 No. 7 1289–1303
www.jcb.org/cgi/doi/10.1083/jcb.201010059

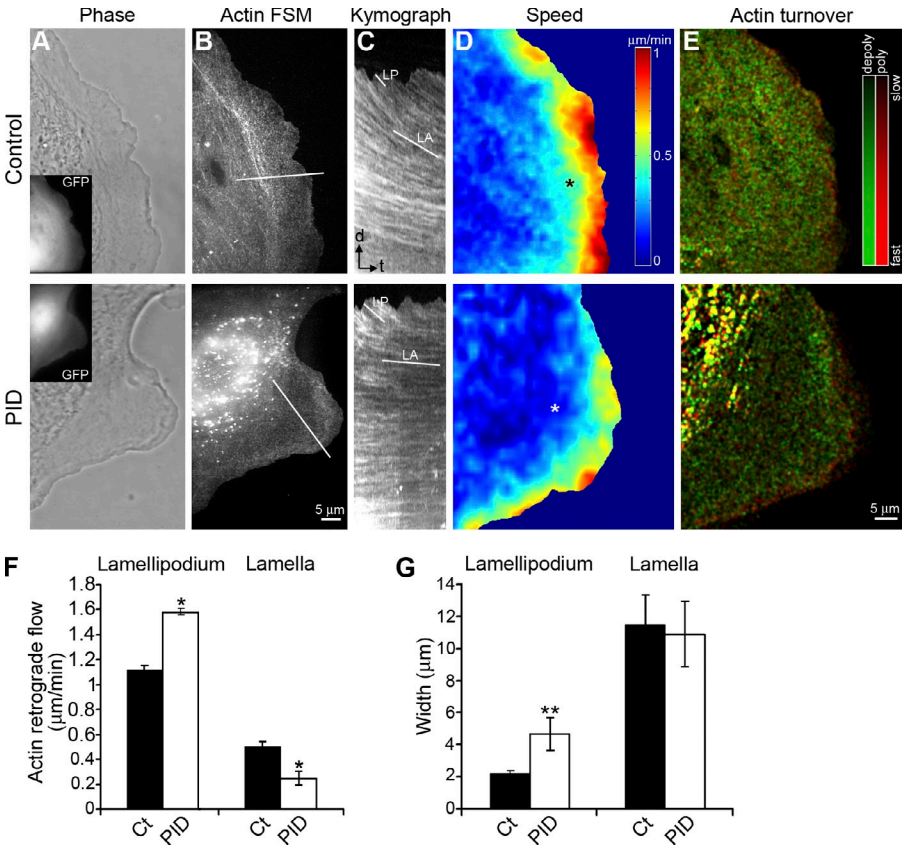

Figure 1. **Pak inhibition decreases F-actin flow and turnover in the lamella.** (A and B) Phase-contrast (A) and FSM images of X-rhodamine actin (B) in motile PtK1 cells expressing PID WT or an inactive mutant of the PID (PID L107F, used as a control). Insets show GFP expression of the GFP–PID WT or GFP–PID L107F constructs. (C) Kymographs taken from lines oriented along the axis of F-actin flow (indicated in B). Lines in C highlight the F-actin flow rates in the lamellipodium (LP) and the lamella (LA). Time bar (t), 2 min; Bar (d), 2 μm. (D) qFSM kinematic maps of the speed of F-actin flow. Note the slower flow in the lamella of the cell treated with PID (white asterisk) compared with the control cell (black asterisk). (E) qFSM kinetic maps of F-actin polymerization (red) and depolymerization (green) rates. Brightness indicates relative rate magnitude. (F) Average rates of F-actin retrograde flow in the lamellipodium and the lamella of Pak-inhibited cells (expressing PID) and control (Ct) cells (expressing an inactive mutant of PID, PID L107F) ± SEM. Pak inhibition significantly increased F-actin flow in the lamellipodium, whereas it significantly decreased the flow in the lamella. *, $P < 0.0001$ versus control cells; Student's *t* test. (G) Average width of cellular regions measured from kymographs ± SEM. **, $P = 0.0008$; Student's *t* test. (F and G) $n \geq 11$ cells for each condition, with a minimum of 125 measurements per condition.

Adhesion to the ECM modulates the activity of the small RhoGTPases RhoA, Rac, and Cdc42 (Cox et al., 2001). Among the downstream effectors of Rac and Ccd42 is the family of Ser/Thr protein kinases known as p21-activated kinases (Paks; Bokoch, 2003). The group 1 Paks 1–3 consist of a C-terminal catalytic domain and an N-terminal regulatory region containing a p21-binding domain for active Rac and Cdc42, a Pak autoinhibitory domain (PID), and multiple Pro-rich protein interaction motifs. Pak activity has been linked to tumor invasiveness and motility of a variety of human cancer cell lines (Kumar et al., 2006), and, more specifically, Pak1 appears to function in regulating the actin cytoskeleton at the leading edge of the cells, where it regulates changes required for the motility in mammalian cells (Sells et al., 1999). Several targets of Paks are directly implicated in regulating cytoskeletal dynamics, including LIM domain kinase 1 (Edwards et al., 1999), which phosphorylates and inactivates cofilin, an F-actin–severing and –depolymerizing protein, or myosin light chain (MLC; Chew et al., 1998) and MLC kinase (Sanders et al., 1999), which control myosin contractility. Paks are also involved in the reorganization of the FAs (Manser et al., 1997; Nayal et al., 2006). Although Paks have been implicated for many years in the regulation of specific aspects of motility through the identification of Pak targets, there has never been any integrated view of the exact nature of the contributions of Pak activity to leading-edge cytoskeletal behavior in the context of motility.

We previously found that Pak1, downstream of Rac, exhibits a region-dependent functionality in regulating F-actin. In the lamellipodium, Pak1 promotes turnover of F-actin via regulation of cofilin phosphorylation, thereby increasing the rate of polymerization-driven retrograde flow (Delorme et al., 2007). In contrast, Pak1 regulates myosin IIA–driven F-actin flow in the lamella via signaling pathways acting independently of cofilin.

Using several quantitative live cell microscopy assays, we describe in detail in this study that the inhibition of Paks abolishes F-actin flow in the lamella, displaces myosin IIA from the cell edge, and decreases FA turnover. By controlling the dynamics of these three systems, Paks regulate the protrusive activity and migration of epithelial cells. Furthermore, we find that expressing Pak1 is sufficient to overcome the inhibitory effects of excess adhesion strength on leading-edge protrusion and cell motility. Collectively, we demonstrate here that Pak1 acts to critically coordinate the relationship between F-actin, myosin IIA, and FA dynamics for efficient cell migration.

Results

Pak inhibition affects F-actin kinetics and kinematics at the cell leading edge

It is well established that actin filaments move from the cell periphery toward the cell center. This F-actin retrograde flow is driven by F-actin polymerization force in the lamellipodium and myosin II activity in the lamella (Ponti et al., 2004). To investigate whether Paks are involved in regulating F-actin flow at the cell leading edge, we performed fluorescent speckle microscopy (FSM) of PtK1 rat-kangaroo kidney epithelial cells, for which F-actin cytoskeleton organization and dynamics have

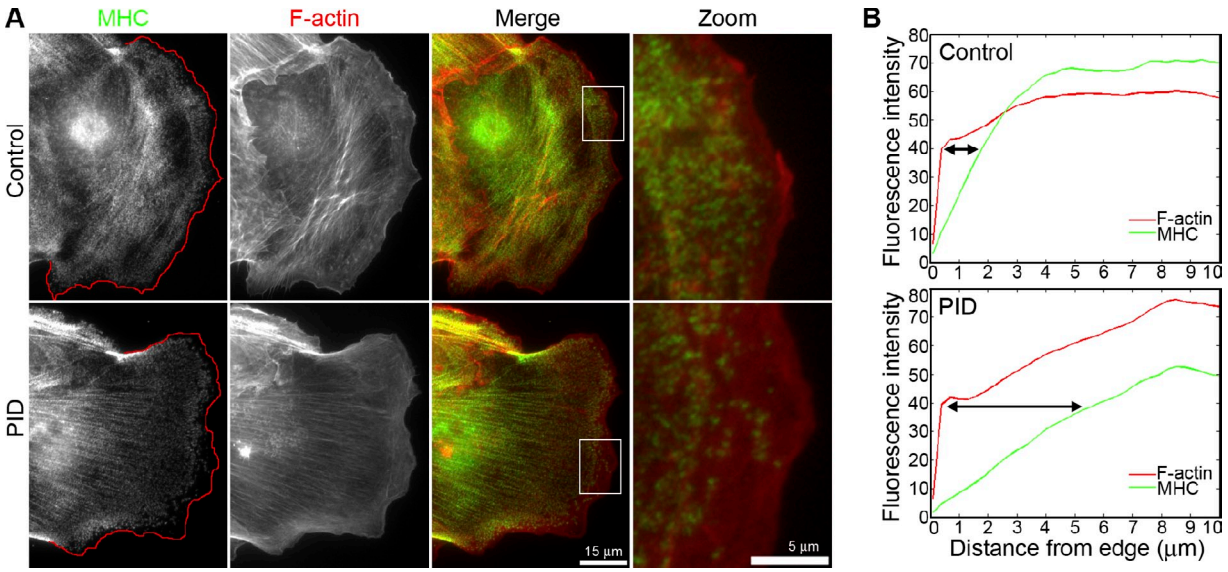

Figure 2. **Pak inhibition displaces myosin IIA from the leading edge.** (A) MHC immunofluorescence (green) and F-actin phalloidin staining (red) in migrating PtK1 expressing PID or an inactive mutant of the PID (PID L107F, noted control). Red lines in the MHC column indicate the leading edge of the cells as determined by the F-actin staining. White boxes in the merge column indicate the positions of insets for higher magnifications shown in the rightmost column. (B) Quantification of fluorescence intensity of MHC and F-actin for each indicated condition, measured from the cell edge (0 µm) into the cell center (10 µm). The data shown represent one experiment and are averaged from $n \geq 14$ cells for each condition. The experiment was repeated at least three times with similar results. The arrows indicate the MHC-depleted zone from the cell edge. MHC was depleted in the first 2 µm in control cells, a distance corresponding to the size of the lamellipodium, whereas it was absent from at least 5 µm in Pak-inhibited cells.

been extensively characterized (Ponti et al., 2004; Gupton et al., 2005; Gupton and Waterman-Storer, 2006). PtK1 cells express both Pak1 and Pak2 (Fig. S1 A). Pak activity was decreased by expressing PID (aa 83–149 of Pak1), which acts as a dominant-negative inhibitor of both Pak1 and Pak2 in vivo (Fig. 1, A–E; and Video 1). Quantitative FSM (qFSM) and kymograph analysis of kinematics revealed that F-actin retrograde flow velocity in the lamellipodium increased upon Pak inhibition (Fig. 1 F). This effect was associated with a widening of the lamellipodium region (Fig. 1 G), as we had previously observed (Delorme et al., 2007). In marked contrast, the F-actin flow rate in the lamella was significantly reduced (Fig. 1, C, D, and F), a phenotype that was reported in Wittmann et al. (2003). We next analyzed the spatial organization of F-actin assembly/disassembly rates. qFSM mapping of F-actin turnover revealed that Pak-inhibited cells were characterized by a well-defined lamellipodium/lamella junction, where the treadmilling lamellipodium was indicated by narrow bands of fast polymerization/depolymerization (Fig. 1 E, bright red and bright green, respectively), whereas the lamella was represented by random foci of weaker assembly/disassembly (Fig. 1 E). In control cells, the lamellipodium was so thin that the integration of all the frames abolished the local polymerization/depolymerization bands. Experiments with the Pak inhibitor IPA-3 supported these conclusions (Fig. S2 and Video 2). Collectively, these results indicate that Pak activity regulates the organization and kinematics of the F-actin cytoskeleton both in the lamellipodium and the lamella.

Pak regulates myosin IIA distribution at the leading edge

Because F-actin kinematics in the lamella are myosin II dependent (Ponti et al., 2004) and Paks are known to regulate myosin II contractility (Bokoch, 2003), we further investigated whether the decreased F-actin flow observed in Pak-inhibited cells could be a result of a change in myosin II distribution and/or activity. Two major isoforms of myosin II have been described, myosin IIA and IIB, that serve different roles in the regulation of the actin cytoskeleton (Vicente-Manzanares et al., 2007). Although myosin IIB localizes in the cell center and the convergence zone, i.e., the region between the lamella and the cell body, myosin IIA is present in the lamella and is involved in the regulation of F-actin retrograde flow (Cai et al., 2006). Immunofluorescence localization of myosin IIA heavy chain (MHC) indicated that myosin was not only absent in the lamellipodium, as previously described (Ponti et al., 2004; Delorme et al., 2007), but was also depleted much beyond the cell edge in the protrusions of Pak-inhibited cells as compared with controls (Figs. 2 A and S3, A and B). These observations were confirmed by quantification of the fluorescence intensity of MHC and F-actin from the leading edge into the cell center (Fig. 2 B). MHC was depleted in the first 2 µm adjacent to the cell edge in control cells, a distance corresponding to the size of the lamellipodium (Fig. 1 G). In contrast, MHC was absent from at least 5 µm from the leading edge in Pak-inhibited cells (Fig. 2 B). Phosphorylated myosin II regulatory light chain (pMLC), an indicator of activated myosin II, was also depleted in the lamella; however, no significant difference in the pMLC/MHC ratio was measured compared with control cells (unpublished data). Collectively, these data indicate that Pak inhibition displaces myosin IIA from the cell leading edge.

Pak inhibition affects the organization and dynamics of paxillin in FAs

F-actin assembly as well as myosin IIA–dependent contractility contribute to the initiation and maturation of adhesion

sites (Giannone et al., 2007). Because both systems were affected upon decreased Pak activity and because Paks are also known regulators of adhesion turnover (Manser et al., 1997; Nayal et al., 2006), we next assessed how Pak inhibition could affect FA morphology. To this end, the FA marker paxillin was localized in cells expressing the PID domain (Fig. 3, A–E; and Fig. S3, C–G). We first confirmed the recruitment of Pak1 into FAs in our cell model and showed that active Pak1 and Pak2 indeed colocalized with paxillin (Fig. S1, B and C). Using total internal reflection fluorescence (TIRF) microscopy, we observed that Pak inhibition induced the formation of long and thin FAs (Fig. 3 A). Quantification of the paxillin foci length revealed that 81.2% of the FAs was longer than 3 µm in cells expressing PID wild type (WT) compared with 34.6% in control cells that expressed PID L107F inactivating mutant (Fig. 3 E). Furthermore, FAs in Pak-inhibited cells were sparsely stained with paxillin (Fig. 3 B) and had a significantly smaller area than that in control cells (Fig. 3 C). Finally, Pak inhibition significantly increased the distribution of FAs throughout the ventral cell surface (Fig. 3 D). To demonstrate more rigorously the role of Paks in FA distribution, we generated double RNAi knockdown of Pak1 and Pak2 in U2OS cells (Fig. 4 A). Immunolocalization of paxillin indicated that FAs in Pak-depleted cells distributed throughout the entire cells (Fig. 4 B) and were less densely stained than those in control cells (Fig. 4 C). Although the average adhesion area in Pak siRNA cells was not different from the one in control cells (Fig. 4 D), the percentage of the ventral surface area containing FAs was increased (Fig. 4 E). Finally, Pak depletion significantly increased paxillin foci length with 49% of FAs longer than 3 µm in Pak knockdown cells compared with 14% of those in siRNA control cells (Fig. 4 F). Collectively, these results confirm the phenotype observed in PtK1 cells upon Pak inhibition and indicate that Paks play a critical role in the regulation of FA distribution.

To next test whether Pak inhibition affected FA kinetics, we imaged migrating cells expressing GFP-paxillin by TIRF microscopy and measured the rates of GFP intensity change in forming or disassembling FAs (Fig. 3, F–I; and Video 3; Webb et al., 2004). This assay revealed that Pak inhibition primarily impaired the rates of FA assembly but also significantly decreased the disassembly rates (Fig. 3 H). FA lifetime was then measured from the first appearance of a resolvable GFP-paxillin cluster until complete disassembly. PID expression significantly increased FA lifetime compared with control cells (Fig. 3 I). In fact, FAs in Pak-inhibited cells never disassembled during the 30 min of imaging.

The absence of cluster formation and the decrease in FA assembly/disassembly rates prompted us to investigate the maturation of FAs in Pak-inhibited cells. The protein zyxin constitutes a distinctive protein marker that localizes to fully grown, mature FAs but not to the nascent focal complexes (Zaidel-Bar et al., 2003). Zyxin localization revealed that the number of mature FAs was significantly decreased upon Pak inhibition (Fig. S4, A and B). Collectively, these results indicate that Pak inhibition induces the formation of elongated FAs with decreased turnover and maturation.

Pak inhibition decreases cell migration and protrusiveness

Cell migration is mediated by the interdependent dynamics of F-actin, myosin II, and FA systems (Gupton and Waterman-Storer, 2006). Our results suggest that Paks play a pivotal role in all three systems; therefore, we investigated the role of Paks in cell protrusion and motility. We first evaluated the effect of Pak inhibition on leading-edge dynamics (Fig. 5, A and B). In control cells, protrusion events propagated as transverse waves along the cell edge (Fig. 5, A, visible as diagonal red stripes) that were interrupted by retraction events (Fig. 5 A, visible as diagonal blue stripes in the top panel; Machacek and Danuser, 2006). In PID-expressing cells, such patterns of coordinated edge movement were dramatically reduced, with very short and disorganized protrusion events (Fig. 5 A, bottom). Determination of the protrusion efficiency showed that only control cell scores were significantly different from 1, indicating a net advancement of the entire leading edge (Fig. 5 B). Pak-inhibited cells did not significantly protrude on average, suggesting that these cells have lost the balance between protrusion and retraction events along the edge (Fig. 5 B). The functional significance of Pak inhibition was next determined by assaying its effects on the migration of epithelial cell islands (Fig. 5, C–G; and Video 4). The migration rates for PID-expressing cells showed a 33% decrease compared with control cells (Fig. 5 G). Analysis of individual cell tracks revealed that Pak-inhibited cells displayed shorter migration paths, with significantly decreased net and total path lengths compared with control cells (Fig. 5, C–E). We conclude that by controlling the organization and dynamics of F-actin, myosin II, and FAs, Paks regulate the protrusive activity and migration of PtK1 cells.

Pak activity is regulated by adhesion strength

In a recent study, adhesion strength, modulated by ECM ligand density, was shown to regulate migration velocity by spatiotemporal feedback between specific parameters of actomyosin and FA dynamics (Gupton and Waterman-Storer, 2006). However, the biochemical basis for this feedback had not been determined. Optimal cell migration speed occurred at intermediate adhesion strength. In contrast, at high adhesion strength, low myosin II activity across the lamella on many F-actin bundles and thin FAs correlated with slow FA turnover and reduced cell migration velocity. Surprisingly, this phenotype was very similar to the one we observed upon Pak inhibition. This prompted us to investigate whether Pak activity was regulated by adhesion strength. 5-, 10-, and 30-µg/ml fibronectin (FN)-coating concentrations were used throughout the study to correspond to low, medium, and high FN, respectively, as described in Gupton and Waterman-Storer (2006). Adhesion of PtK1 cells to high FN concentration decreased Pak phosphorylation, indicative of its activity, compared with cells plated at low and medium adhesion strength (Fig. 6 A). Next, to determine the localization of the active pool of Pak1 and Pak2, PtK1 cells were plated on increasing concentrations of FN, and phosphorylated Pak (pPak) was detected by immunostaining. Active Paks were mainly localized at adhesion sites, as observed by epifluorescence and

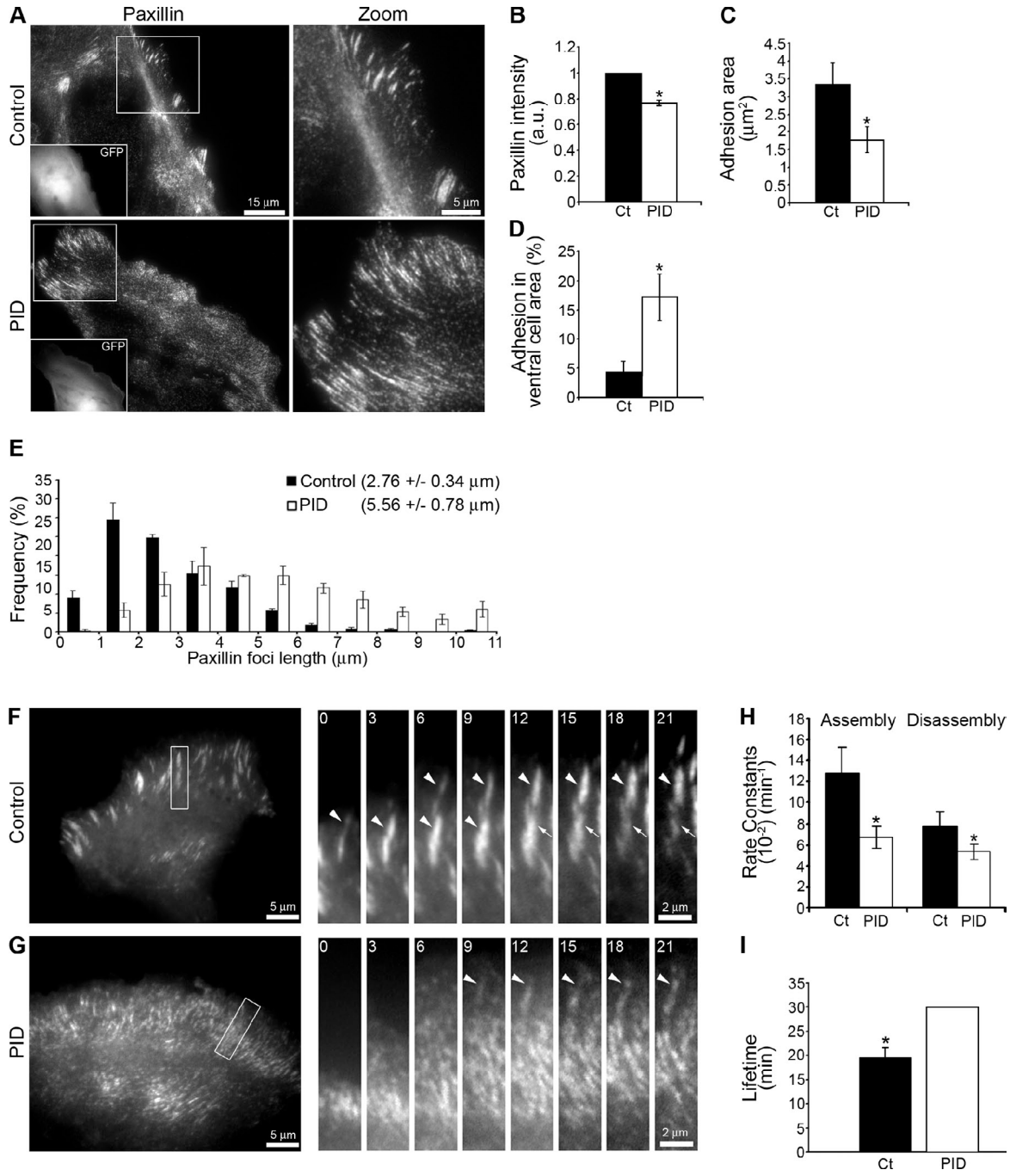

Figure 3. **Pak inhibition affects the organization and dynamics of paxillin in FAs.** (A) Paxillin immunofluorescence imaged by TIRF microscopy in migrating PtK1 cells expressing PID WT or an inactive mutant of the PID (PID L107F, noted control). Insets show GFP expression of the GFP–PID WT or GFP–PID L107F constructs. White boxes in the paxillin column indicate the positions of insets for higher magnifications shown in the right column. (B–D) Quantification of paxillin fluorescence intensity in the protrusion (B), the average adhesion area in the protrusion (C), and the percentage of ventral cell area containing paxillin (D) for each condition ± SEM. *, $P < 1.10^{-6}$ compared with control (Ct) cells; Student's *t* test. a.u., arbitrary units. (E) Frequency histogram of paxillin foci length for each condition ± SEM. Numbers at the top right are the average lengths of the adhesion sites ± SEM. For quantifications in B–E, the experiment was repeated at least three times with $n \geq 30$ cells for each condition, and all detectable FAs were quantified in each cell (corresponding to a minimum of 30 FAs per cell). (F and G) Example of GFP-paxillin fluorescence time-lapse images imaged by TIRF microscopy in PtK1 cells expressing GFP-paxillin alone (noted as a control; F) or in combination with PID (G). White boxes in the whole area images (left) indicate the localization of the magnified regions shown in the right panels. Elapsed time in minutes is shown. Arrowheads and arrows indicate assembling and disassembling FAs, respectively. Note that FAs in Pak-inhibited cells (G) were sparsely stained and assembled/disassembled slower than those in control cells (F). (H) Average rate constants of FA assembly and disassembly measured from 8–15 FAs per cell ± SEM, and $n \geq 7$ cells per condition. *, $P < 1.10^{-5}$ compared with control cells; Student's *t* test. (I) Average FA lifetime measured from the initiation of a new GFP-paxillin cluster to complete disappearance (±SEM). *, $P < 1.10^{-6}$ compared with PID-expressing cells. FAs in PID-expressing cells never disassembled during the 30 min of imaging.

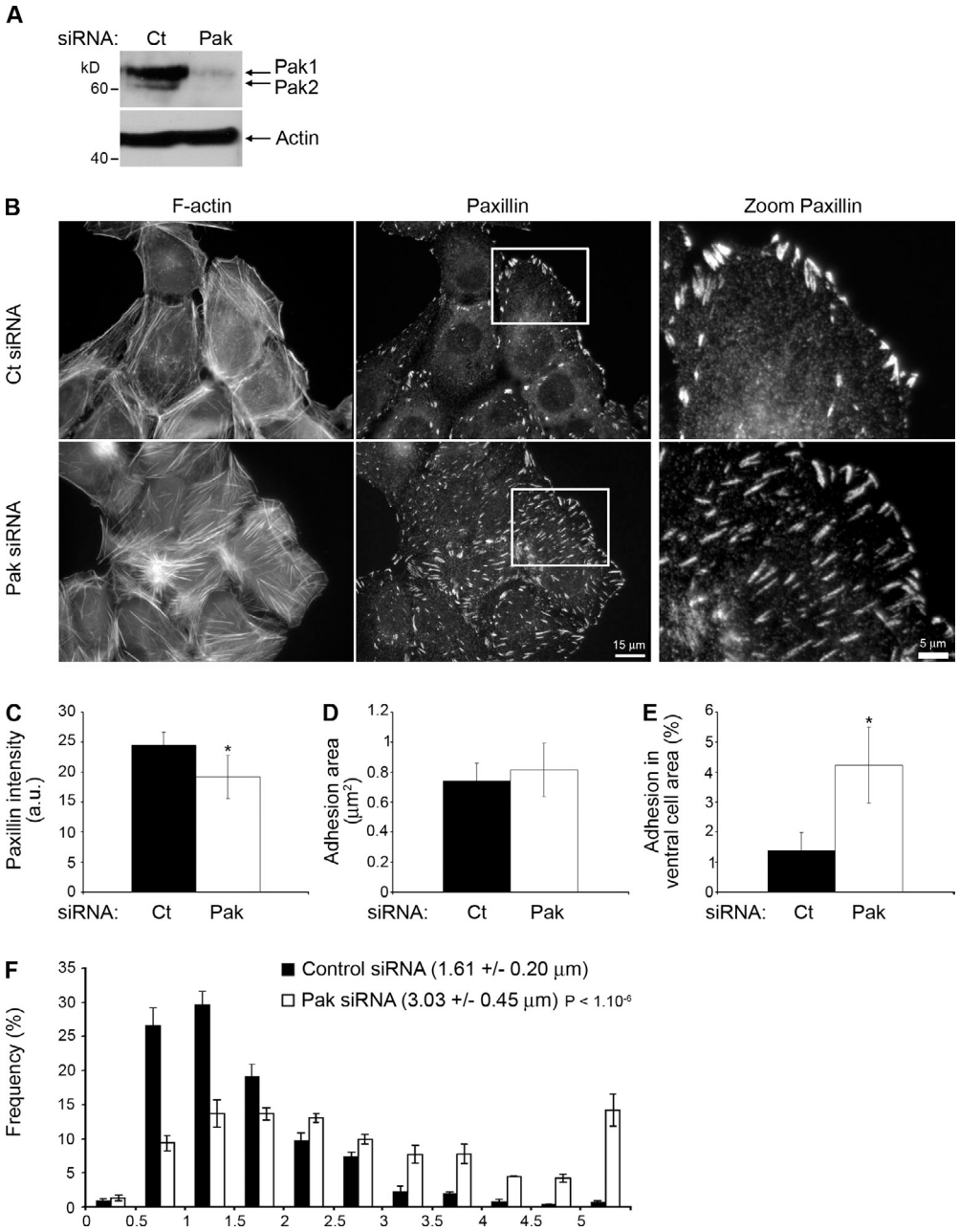

Figure 4. **Pak depletion affects FA distribution.** (A) Immunoblot of Pak1 and Pak2 in U2OS cells transfected for 72 h with control (noted as Ct) siRNA or with siRNAs targeting Pak1 and Pak2 (noted as Pak). The actin immunoblot was used as a loading control. (B) Immunofluorescence of paxillin and F-actin staining in U2OS cells transfected for 72 h with control siRNA (noted as Ct siRNA) or siRNAs targeting Pak1 and Pak2 (noted Pak siRNA). White boxes in the paxillin column indicate the positions of insets for higher magnifications shown in the right column. (C–E) Quantification of paxillin fluorescence intensity in the protrusion (C), the average adhesion area in the protrusion (D), and the percentage of ventral cell area containing paxillin (E) for each siRNA condition ± SEM. *, $P < 1.10^{-6}$ compared with control siRNA; Student's *t* test. a.u., arbitrary units. (F) Frequency histograms of paxillin foci length for control cells or cells depleted in Pak (±SEM). The numbers at the top right are the average lengths of the adhesion sites ± SEM. For quantifications in C–F, the experiment was repeated at least three times with $n \geq 30$ cells for each condition, and all detectable FAs were quantified in each cell (corresponding to a minimum of 30 FAs per cell).

TIRF microscopy (Fig. 6 B and Fig. S5 A, respectively). As shown in Fig. 6 C, quantification of pPak fluorescence intensity in the FAs revealed that 49.8% of FAs at high adhesion strength (FN30) had a pPak fluorescence intensity <100 compared with 20.9% of FAs at low adhesion strength (FN5). In contrast, only 1.8% of FAs in cells plated on FN30 presented a high Pak activity (fluorescence intensity >400) compared with 12.6% of adhesions in cells at low adhesion strength. Together, our data demonstrate that the level of Pak activity in FAs is inversely correlated with FN density.

Expression of Pak1TE can rescue F-actin phenotypes at high adhesion strength

Our results suggest Paks to be the critical biochemical link between ECM density and actin dynamic behavior to control rates of cell migration. Because we found that the active Pak level is

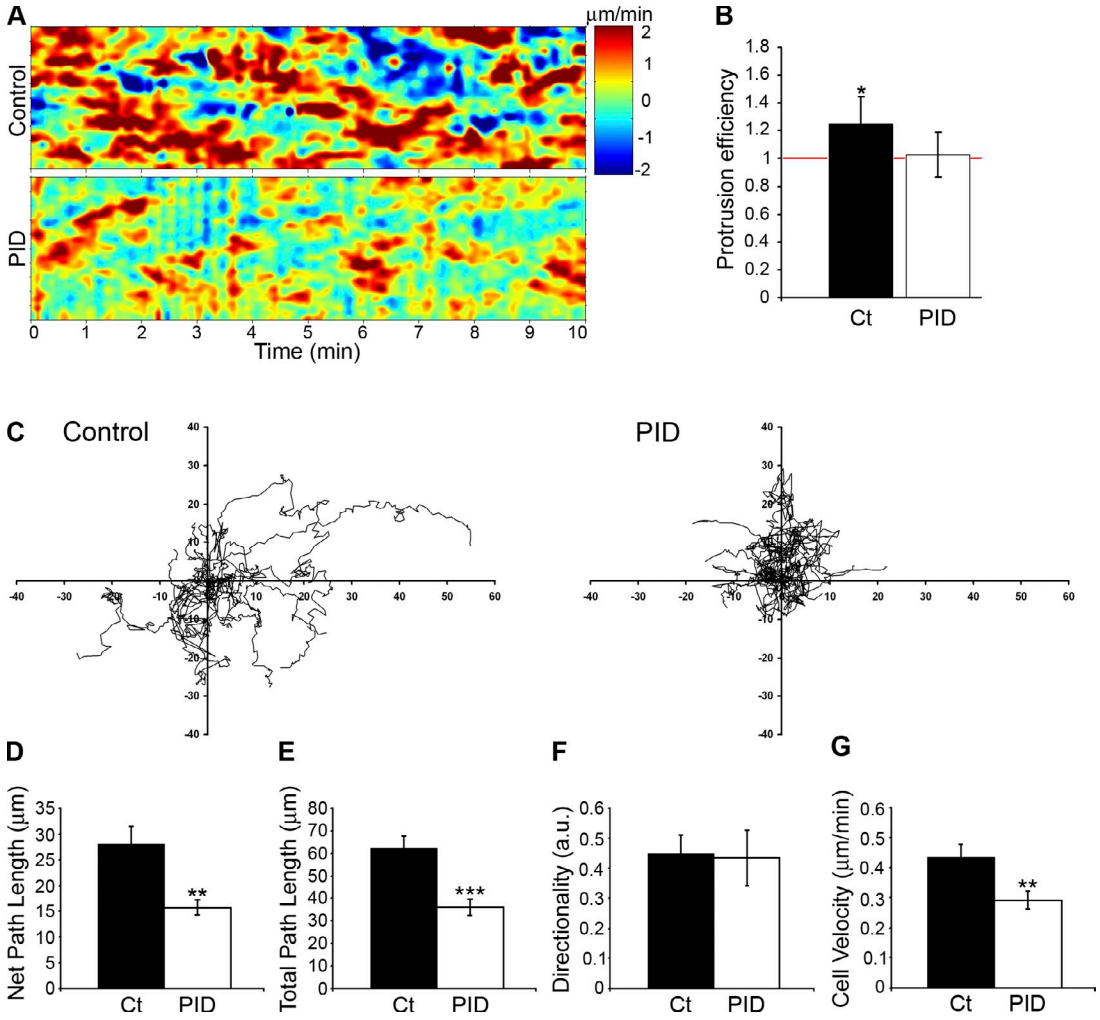

Figure 5. **Pak inhibition decreases cell migration and protrusiveness.** (A) Activity maps of cell edge movement over time in migrating PtK1 cells expressing PID or an inactive mutant of the PID (PID L107F, noted as control). Edge displacements are encoded with warm color (red) for protrusion and cold color (blue) for retraction. (B) Average protrusion efficiency ± SEM. A protrusion efficiency value >1, represented by the red line, indicates a net advancement of the entire leading edge. Pak-inhibited cells did not protrude efficiently (P = 0.95 for PID-expressing cells). $n \geq 7$ cells for each condition. *, P < 0.05 compared with a protrusion efficiency of 1. (C) Individual tracks of 15 cells expressing PID L107F as a control or PID WT transposed to a common origin. Pak inhibition led to shorter migration paths. (D–G) Quantification of motility parameters in C, including net path length (D), the net distance that the cells traversed from the first to the last frame; total path length (E), the total distance traversed by cells over time; directionality (F), the ratio of net to total path length; and cell velocity (G). The experiment was repeated at least four times, and $n \geq 30$ cells analyzed for each condition. **, P < 0.01; ***, P = 0.0001 compared with control (Ct) cells. a.u., arbitrary units.

decreased in cells migrating at high adhesion strength, we investigated whether expressing Pak1 in these cells would phenocopy cells migrating at lower adhesion strength. qFSM analysis of F-actin was performed on cells plated on high FN concentration and expressing Pak1 T423E (noted as Pak1TE; Fig. 7, A–E; and Video 5). This mutant is widely used as a model for activated Pak1 (Sells et al., 1997, 1999; Bagheri-Yarmand et al., 2000), although a recent study has questioned its constitutive activity (Ng et al., 2010). Remarkably, cells expressing Pak1TE displayed an actin dynamics phenotype similar to the one observed in cells migrating on uncoated coverslips (compare Fig. 7 [A–E] with Fig. 1 [A–E]). Specifically, compared with control cells at high adhesion strength, cells expressing Pak1TE had slower F-actin flow rates in the lamellipodium, which is associated with decreased width of this region, whereas F-actin flow rates in the lamella were significantly faster (Fig. 7, F and G). Thus, expression of Pak1TE is sufficient to rescue F-actin kinetics at high adhesion strength.

Expression of Pak1TE can rescue myosin IIA distribution and FA dynamics at high adhesion strength

Next, to determine whether increased actin retrograde flow in the lamella promoted by expression of Pak1TE correlated with a specific myosin IIA and FA dynamic organization, we localized myosin IIA and paxillin in cells plated at high adhesion strength and expressing Pak1TE. Immunofluorescence localization of pMLC revealed that myosin IIA localized closer to the leading edge in the protrusion of cells with enhanced Pak1 compared with control cells (Fig. 8, A and B).

Analysis of paxillin immunofluorescence established that expressing Pak1TE at high adhesion strength generated shorter

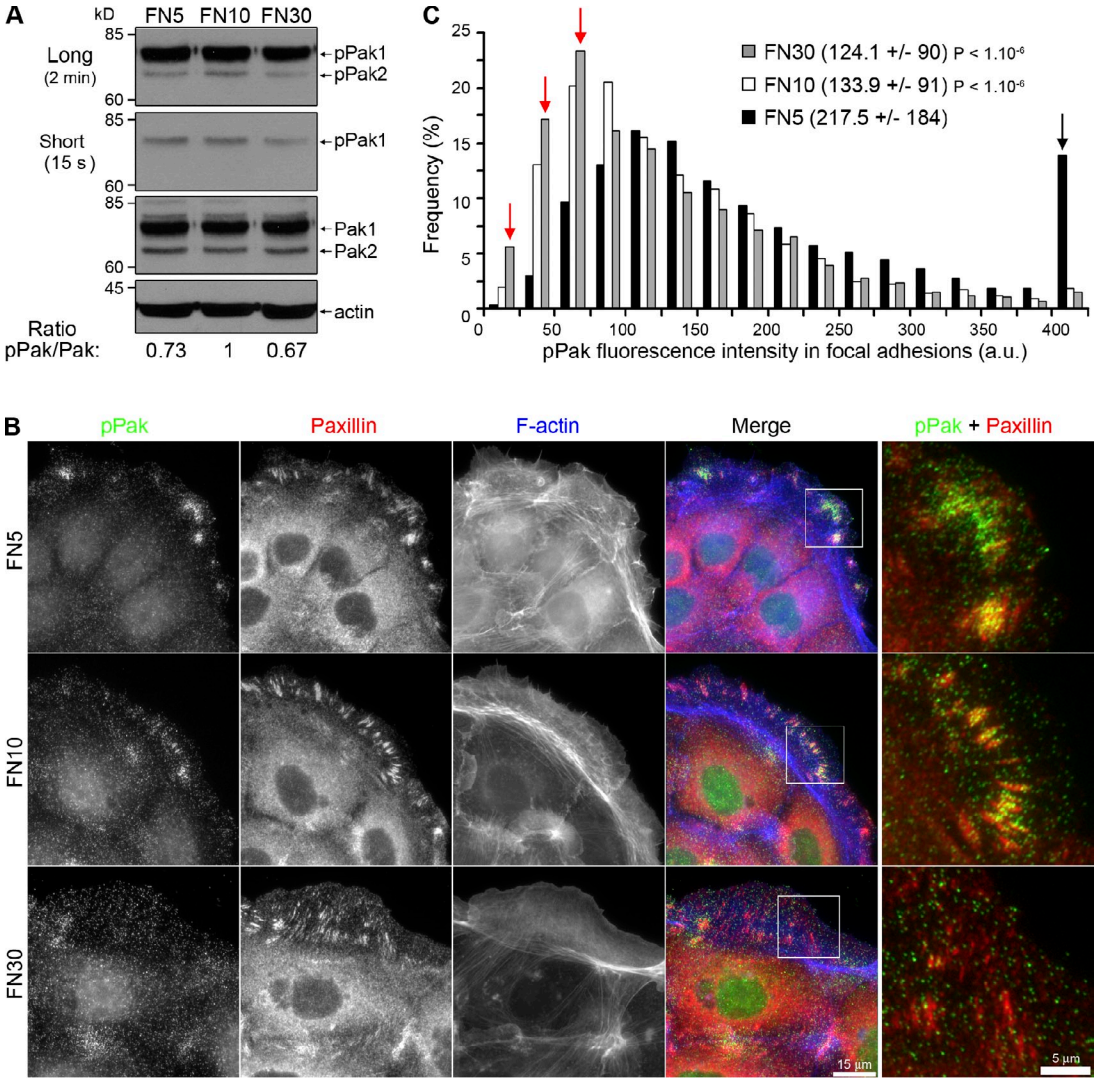

Figure 6. **Pak activity is regulated by adhesion strength.** (A) Cell lysates from PtK1 cells plated on low (5 µg/ml, FN5), medium (10 µg/ml, FN10), or high (30 µg/ml, FN30) FN concentrations were analyzed by immunoblotting and probed with phospho-specific antibodies anti-Pak1/Pak2 (active Pak1/Pak2) and antibodies to total proteins anti-Pak1/Pak2 and anti-actin. Two exposure times of the same immunoblot are shown: long (2-min exposition) and short (15-s exposition). Quantification of immunoblots was determined by the ratio of phosphorylated to total Pak1/Pak2 and was normalized to the FN10 condition, which correlates with optimal cell migration. The values shown are averages of three independent experiments. (B) Immunofluorescence with antibody directed against active Paks (pPak), paxillin, and F-actin phalloidin staining in PtK1 cells plated on FN5, FN10, and FN30. White boxes in the merge column indicate the positions of insets for higher magnifications shown in the rightmost column. (C) Frequency histogram of pPak fluorescence intensity in FAs for each FN concentration (low FN5, medium FN10, and high FN30). The numbers at the top right are the average pPak intensities ± SD. The data shown are representative of one experiment and are averaged from $n \geq 30$ cells for each condition. The experiment was repeated three times with similar results. All detectable FAs were quantified in each cell (corresponding to a minimum of 30 FAs per cell). The red arrows indicate the increased frequency of FAs containing a low pPak level observed in cells plated at a high adhesion strength (FN30). In contrast, the black arrow indicates the increased frequency of FAs containing a high pPak level observed in cells plated at a low adhesion strength (FN5).

but more dense FAs and promoted a more peripheral localization compared with control cells (Fig. 9 A). Furthermore, time-lapse imaging of cells plated at high adhesion strength and expressing GFP-paxillin revealed that Pak1TE expression increased both FA assembly and disassembly rates (Fig. 9, B and C). We also observed some FAs completely turning over during the period of imaging, whereas most FAs in control cells never disassembled during the same period (Fig. 9 D and Video 6). Finally, we investigated the effect of adhesion strength on the maturation of FAs. Zyxin localization indicated that FA maturation was inversely correlated with ECM concentration: i.e., high levels of zyxin in FAs at low adhesion strength and low levels of zyxin at high FN concentration. Pak1TE expression in cells plated at high adhesion strength partially rescued the maturation of FAs compared with control cells (Fig. S4, C and D). Collectively, these data suggest that expressing Pak1TE in cells plated at high FN concentration promotes myosin contractility and FA growth, which in turn generates a specific F-actin phenotype.

Expression of Pak1TE recapitulates protrusiveness and rapid migration at nonoptimal ECM density

Because the specific F-actin dynamics, myosin IIA, and FA distribution observed at high adhesion strength were associated

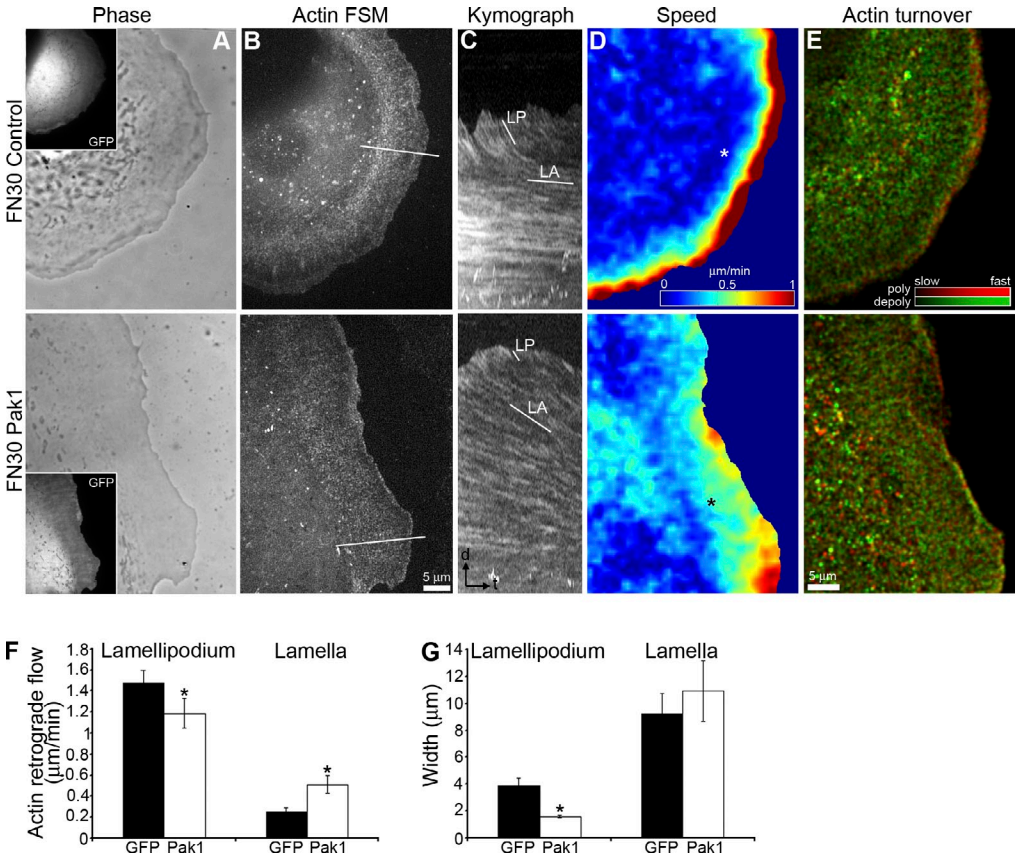

Figure 7. **Pak1TE expression rescues F-actin phenotypes at a high adhesion strength.** (A and B) Phase-contrast (A) and FSM images of X-rhodamine actin (B) in migrating PtK1 cells plated at high FN concentration (30 μg/ml) and expressing GFP alone (noted as FN30 control) or GFP–Pak1TE (noted as FN30 Pak1). Insets show GFP expression of the GFP or GFP-Pak1TE constructs. (C) Kymographs taken from lines oriented along the axis of F-actin flow (indicated in B). The lines in C highlight the F-actin flow rates in the lamellipodium (LP) and the lamella (LA). Time bar (t), 2 min; Bar (d), 2 μm. (D) qFSM kinematic maps of the speed of F-actin flow. Note the increased flow in the lamella of the cell expressing Pak1TE (black asterisk) compared with the control cell (white asterisk). (E) qFSM kinetic maps of F-actin polymerization (red) and depolymerization (green) rates. Brightness indicates relative rate magnitude. (F) Average rates of F-actin retrograde flow in the lamellipodium and the lamella of control and Pak1TE-expressing cells ± SEM. The expression of Pak1TE significantly decreased F-actin flow in the lamellipodium, whereas it significantly increased the flow in the lamella (*, $P = 0.002$ and *, $P < 1.10^{-5}$, respectively, compared with control cells; Student's *t* test). (G) Average width of cellular regions measured from kymographs ± SEM. Pak1TE expression decreased lamellipodium width. *, $P < 1.10^{-5}$ compared with control; Student's *t* test. (F and G) $n \geq 9$ cells were analyzed for each condition, with a minimum of 125 measurements per condition.

with slow migration, we then sought to determine whether enhancing Pak1 would promote leading-edge dynamics and rapid migration. In cells expressing Pak1TE, patterns of coordinated leading-edge movements were increased, with longer waves of positive velocities propagating along the cell edge (Fig. 10 A). As a result, protrusion efficiency was >1 in these cells, indicating a net advancement of the leading edge, in contrast to control cells that did not significantly protrude on average when migrating at high adhesion strength (Fig. 10 B). Next, we assayed the effects of Pak1TE expression on cell motility (Video 7). Analysis of individual cell tracks revealed that cells expressing Pak1TE displayed longer migration paths than control cells (Fig. 10 C). Consistent with this analysis, these cells showed significant differences in both net and total path lengths (Fig. 10, D and E). Consequently, directionality was higher (Fig. 10 F). Finally, Pak1TE expression at high adhesion strength significantly increased cell migration velocity by 46% compared with control cells (Fig. 10 G). Interestingly, expression of a kinase-defective Pak1 (Pak1 K299R) in cells plated at high FN concentration did not rescue cell migration parameters compared with control cells (Fig. S5, B–F). Thus, the Pak1TE mutant significantly behaves differently than the kinase-dead Pak1 and is sufficient to overcome the inhibitory effects of excess adhesion strength on leading-edge protrusion and cell migration.

Discussion

The dependence of migration speed on increasing adhesion strength was predicted long ago by mathematical modeling (DiMilla et al., 1991) and was experimentally verified, for example, by modulating ECM ligand density (Palecek et al., 1997). Although it was long thought to be a simple consequence of mechanical effects of adhesion strength, a more recent study demonstrated that adhesion strength maximizes migration speed by optimizing the dynamic organizational state of the F-actin, myosin IIA, and FA networks within the cell leading edge (Gupton and Waterman-Storer, 2006). These results have been recently confirmed by a computational modeling that incorporates molecular mechanisms of ECM-mediated signaling (Cirit et al., 2010). What has remained unknown is the biochemical

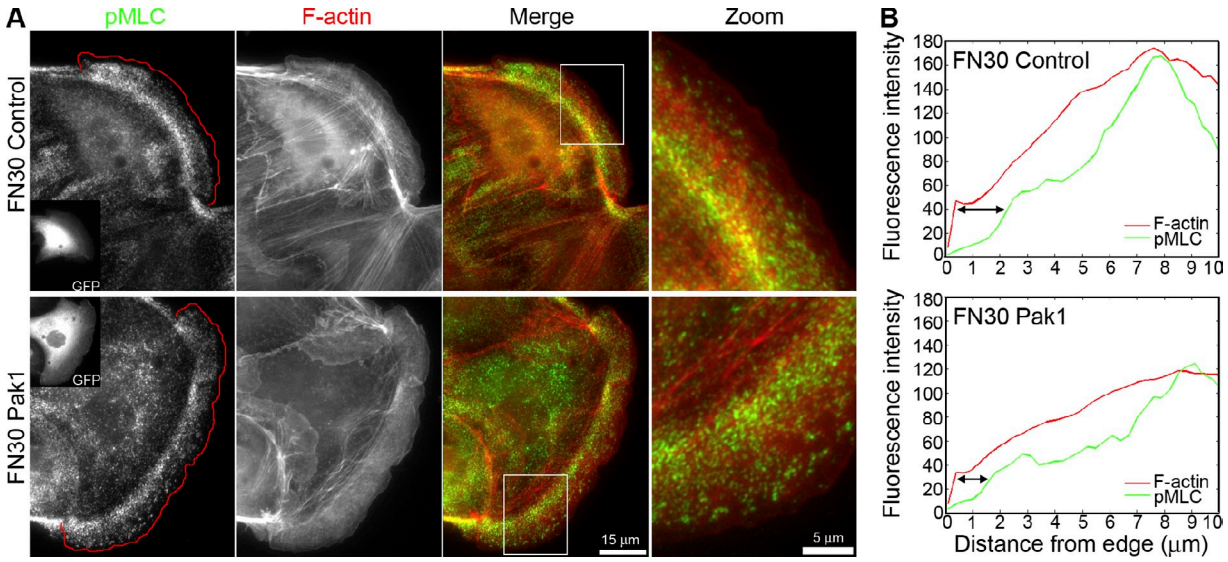

Figure 8. **Pak1TE expression rescues myosin IIA distribution at a high adhesion strength.** (A) pMLC immunofluorescence and F-actin phalloidin staining in migrating PtK1 cells plated on high FN concentration (30 µg/ml) and expressing GFP (noted FN30 control) or GFP–Pak1TE (noted FN30 Pak1). Insets in pMLC column show GFP expression of the GFP or GFP-Pak1TE constructs. Red lines indicate the leading edge of the cells as determined by the F-actin staining. White boxes in merge column indicate the positions of insets for higher magnifications shown in the rightmost column. (B) Fluorescence intensity of pMLC and F-actin for each indicated condition, measured from the cell edge (0 µm) into the cell center (10 µm). The data shown represent one experiment and are averaged from $n \geq 7$ cells for each condition. The experiment was repeated at least three times with similar results. The arrows indicate the myosin IIA–depleted zone from the cell edge.

link from ECM to adhesion turnover, myosin IIA activity, and F-actin organization. The data presented here suggest that Paks (Pak1 and/or Pak2) critically contribute to this pathway by spatially and temporally organizing the interplay between actin, myosin, and FA dynamics to achieve an optimal balance between adhesion and contraction for maximal cell migration (Fig. 10 H). Our results, along with our earlier observations that Pak1 plays a key role in coupling the functioning of the leading-edge lamellipodia and lamella actin networks (Delorme et al., 2007), place Paks as a crucial biochemical node in RhoGTPase signaling to coordinate cell motility.

When Pak function is inhibited, F-actin retrograde flow is markedly reduced in the lamella. Even though we can't exclude a direct effect of Pak inhibition on actin-binding proteins in this region via yet unidentified signaling pathways, our results suggest that the decreased flow rate results from Pak action on myosin contractility and/or FA dynamics. Activation of myosin IIA by phosphorylation of its regulatory light chain is one of the main factors involved in the regulation of cytoskeletal dynamics. It is still controversial under what conditions expression or activation of Paks increases myosin phosphorylation: although Paks can directly phosphorylate MLC (Chew et al., 1998; Kiosses et al., 1999; Sells et al., 1999; Zeng et al., 2000; Brzeska et al., 2004), Paks can also phosphorylate and inactivate MLC kinase and thereby reduce MLC phosphorylation (Sanders et al., 1999; Goeckeler et al., 2000). Recent data indicate that expression of the catalytic domain of ameba Pak in HeLa cells induced direct phosphorylation of MLC and was sufficient to cause disassembly of FAs and stress fibers in the cell center and accumulation of FAs and F-actin at the cell periphery (Szczepanowska et al., 2006). Furthermore, Pak2 was recently found to bind myosin 18A, an emerging member of the myosin superfamily that was reported to lead to MLC phosphorylation, myosin IIA–dependent actomyosin assembly in the lamella, and regulation of F-actin retrograde flow, leading-edge protrusion, and cell motility (Hsu et al., 2010). In our study, we were not able to detect a significant difference in MLC phosphorylation upon Pak inhibition. However, we observed a major depletion of myosin IIA throughout large parts of the protrusion in Pak-inhibited cells. This displacement of myosin from the cell edge could be a result of the widening of the lamellipodium and the increase in cofilin activity (Delorme et al., 2007). The loss of myosin in the protrusion might then contribute to the decreased dynamics/turnover of FAs in Pak-inhibited cells.

Although the formation of nascent focal complexes is myosin IIA independent, the formation of fully developed, mature FAs requires myosin IIA motor activity (Choi et al., 2008). Mature adhesions are thought to transmit strong forces between the cytoskeleton and the ECM (Galbraith et al., 2002) to promote adhesion turnover in cell migration (Webb et al., 2004; Zaidel-Bar et al., 2007). We suggest that decreased FA maturation and turnover in Pak-inhibited cells might result from the depletion of myosin IIA and leads to the inhibition of cell migration. One might also consider a direct effect of Paks on FA dynamics. It is well established that integrin engagement to the ECM leads to Pak activation and the targeting of Paks to adhesion complexes at the cell edge (Manser et al., 1998; del Pozo et al., 2000; West et al., 2001). Pak activity promotes the disassembly of FAs (Zhao et al., 2000), which can be blocked by the Pak inhibitory domain (Manser et al., 1998). More recently, active Pak1 was shown to phosphorylate paxillin Ser^{273}, which in turn increases adhesion turnover, leading-edge protrusion, and cell migration (Nayal et al., 2006). Interestingly, in endothelial cells, both kinase-dead and kinase-active Pak1 stabilize FAs

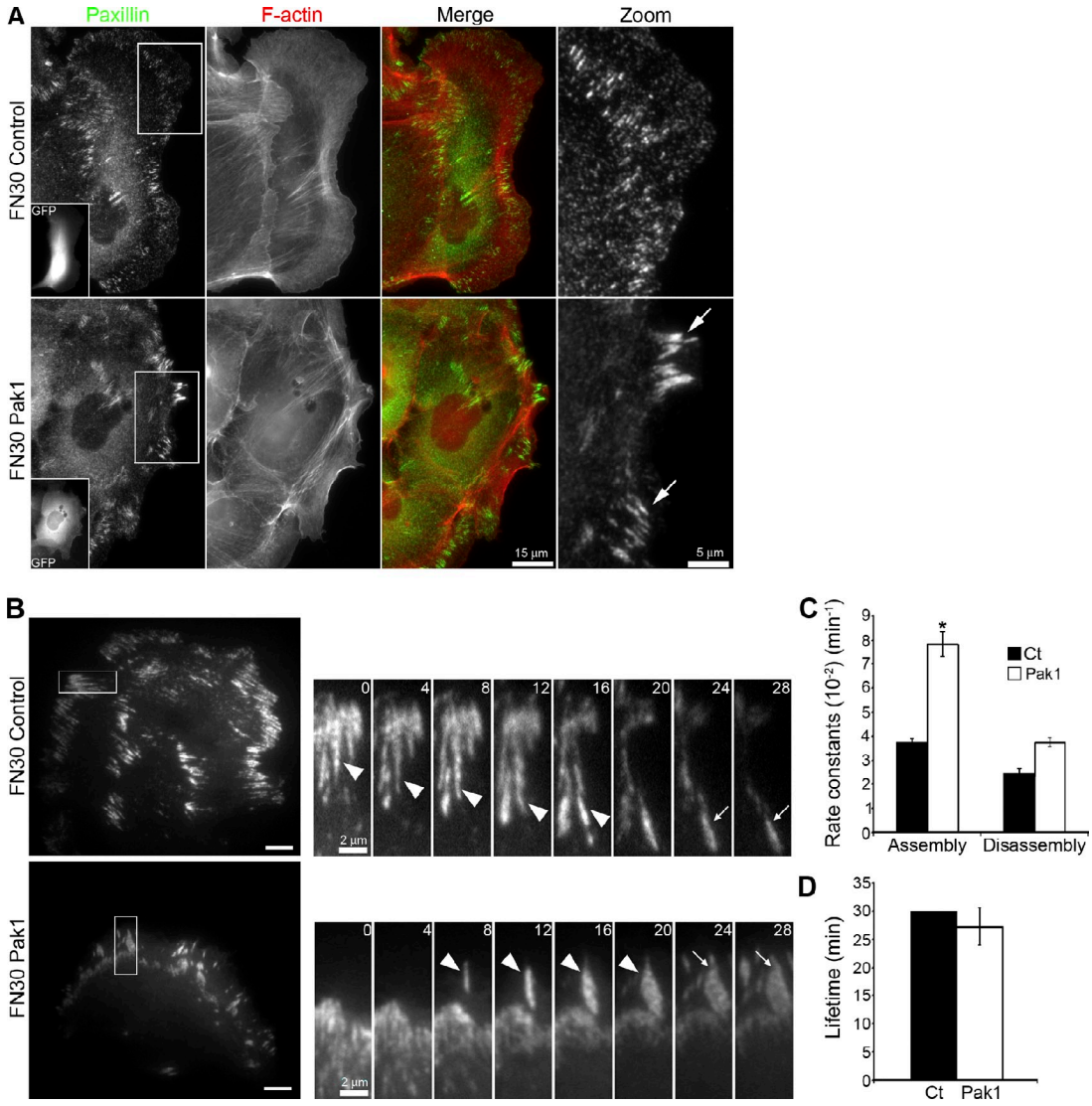

Figure 9. **Pak1TE expression rescues FA distribution and dynamics at a high adhesion strength.** (A) Paxillin immunofluorescence and F-actin phalloidin staining in migrating PtK1 cells plated on high FN concentration (30 µg/ml) and expressing GFP (noted FN30 control) or GFP–Pak1TE (noted FN30 Pak1). Insets show GFP expression of the constructs. White boxes in the paxillin column indicate the positions of insets for higher magnifications shown in the rightmost column. Pak1TE expression induced the formation of thick paxillin clusters (arrows). (B) An example of GFP-paxillin fluorescence time-lapse images taken in PtK1 cells plated on FN30, control, or expressing Pak1TE. The white boxes in the whole area images (left) indicate the localization of the magnified regions shown in the right panels. Elapsed time in minutes is shown. Arrowheads and arrows indicate assembling and disassembling FAs, respectively. Note that FAs in control cells were sparsely stained and assembled/disassembled slower than those in cells expressing Pak1TE. Bars (left), 5 µm. (C) Average rate constants of FA assembly and disassembly measured from 8–15 FAs per cell ± SEM, and $n \geq 6$ cells per condition. *, P = 0.018 compared with control; Student's *t* test. (D) Average FA lifetime measured from the initiation of a new GFP-paxillin cluster to complete disappearance (±SEM). Although FAs in control (Ct) cells never disassembled in the 30 min of imaging, some clusters of paxillin in Pak1TE-expressing cells did completely turn over during this period.

(Kiosses et al., 1999). Thus, there is not a simple correlation between the effects of Paks on FA formation and Pak activity. Overall, we observed that inhibition of Pak activity decreases FA turnover and significantly reduces the dynamics of edge movements and cell motility. Our data are in concordance with a previous study indicating that cells expressing a kinase-dead form of Pak1 displayed a reduced persistence of movement (Sells et al., 1999). Recently, Pak1 activity was described at nascent protrusions at the front lamellipodium in normal rat kidney cells during directional cell migration (Parrini et al., 2009), thus supporting a role of Paks during the early steps of cell migration.

Dynamic changes in the cytoskeleton are necessary for cell migration, and cancer cells are dependent on motility for invasion and metastasis. It is well established that the signaling pathways behind the reshaping and migrating properties of the cytoskeleton in cancer cells involve Paks (Dummler et al., 2009). Indeed, deregulation of Pak activities and expression levels has been implicated in a variety of human cancers such as breast, ovary, colorectal, thyroid, and pancreatic (Carter et al., 2004; Stofega et al., 2004; Kumar et al., 2006). Interestingly, endogenous active Pak1 and Pak2 constitutively localize to large atypical FAs in breast cancer cell lines (Stofega et al., 2004). Overexpression of kinase-dead Pak1 in the highly metastatic MDA-MB-435 breast carcinoma cell line decreased cell motility and invasion, concomitant with an increase in focal contacts and stress fiber formation (Adam et al., 2000). Together, these studies suggest

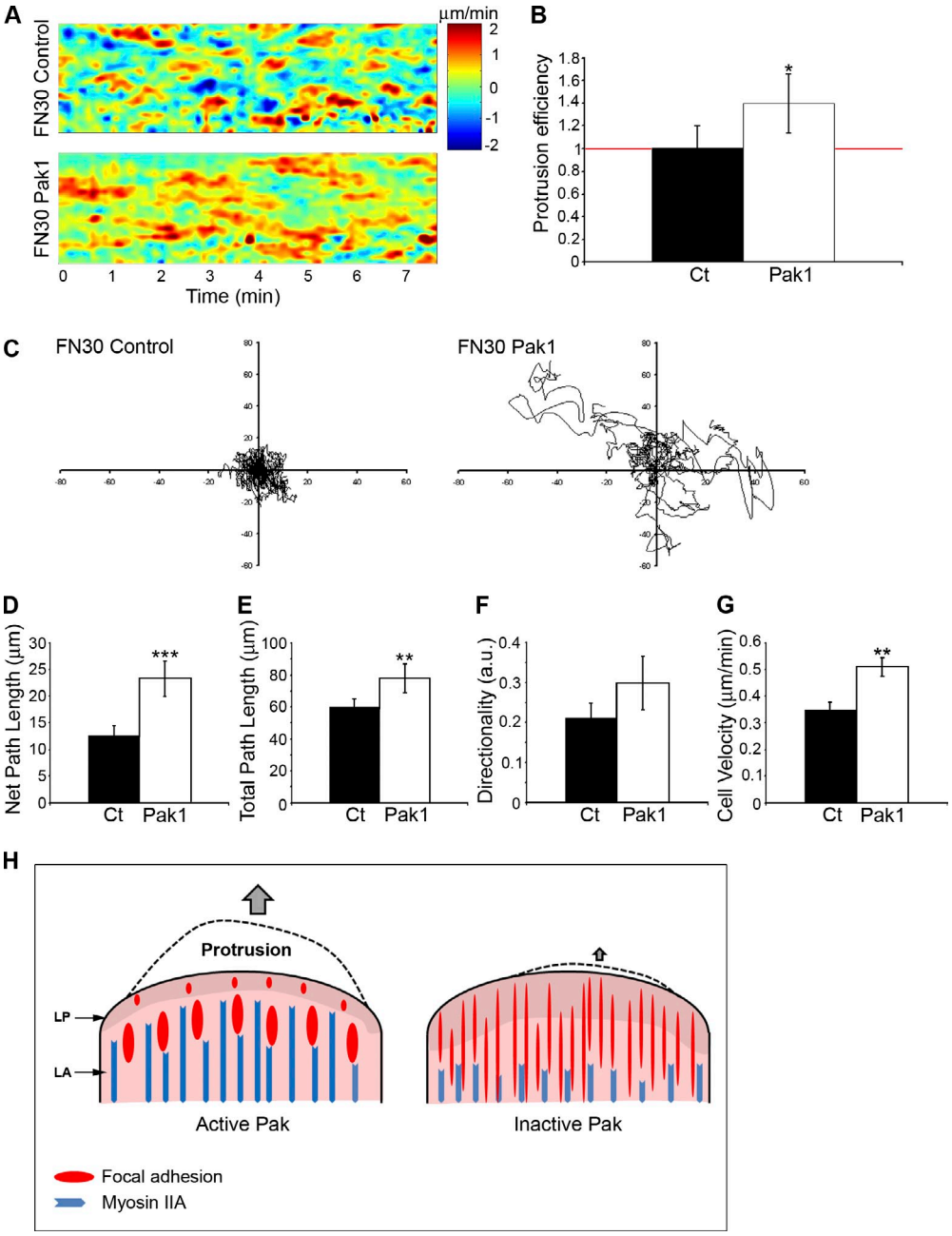

Figure 10. **Pak1TE expression recapitulates protrusiveness and rapid migration at nonoptimal ECM density.** (A) Activity maps of cell edge movement over time in migrating PtK1 cells plated at high FN concentration (30 µg/ml) and expressing GFP alone (noted FN30 control) or GFP–Pak1TE (noted FN30 Pak1). Edge displacements are encoded with warm color (red) for protrusion and cold color (blue) for retraction. (B) Average protrusion efficiency ± SEM. $n \geq 5$ cells for each condition. *, $P < 0.05$ compared with a protrusion efficiency of 1. A protrusion efficiency value >1, represented by the red line, indicates a net advancement of the entire leading edge. (C) Individual tracks transposed to a common origin of 15 cells plated on FN30 and expressing GFP–Pak1TE (noted FN30 Pak1) or not (noted FN30 control). Pak1TE expression led to longer migration paths. (D–G) Quantification of motility parameters in C, including net path length (D), the net distance that the cells traversed from the first to the last frame; total path length (E), the total distance traversed by cells over time; directionality (F), the ratio of net to total path length; and (G) cell velocity. The experiment was repeated at least four times, and $n \geq 17$ cells analyzed for each condition. **, $P < 0.05$ and ***, $P = 0.001$ compared with control (Ct) cells. a.u., arbitrary units. (H) A model of Pak regulation of FA and actomyosin organization. In the presence of active Pak (left), lamellipodium (LP) and lamella (LA) networks present little overlap within the tip of the lamella, adjacent to the cell edge. Myosin IIA is distributed throughout the lamella. FAs appear at the cell edge, mature in the lamella, and disassemble. Coordination between actin dynamics, myosin IIA contractility, and FA turnover leads to efficient protrusion and cell migration. Inhibition of Pak activity (right) widens the lamellipodium and accelerates its F-actin treadmilling rate. In contrast, F-actin retrograde flow in the lamella is inhibited. Myosin IIA is displaced from the leading edge, and FA maturation is decreased. Thus, Pak inhibition reduces the dynamics of edge movements and cell motility.

that Pak1 is a major driver underlying cancer cell migration, and it appears promising to consider Paks as a potential therapeutic target for interrupting cancer progression. Effective targeting of Paks depends on our knowledge of Pak activation and its impact on downstream signaling cascades leading to phenotypic changes relevant to tumor development and progression. In this study, we have described in detail how Paks control the dynamics of actin, myosin, and FAs, thus regulating the protrusive activity and

migration of epithelial cells. These findings establish Paks as critical molecules coordinating cytoskeletal systems for efficient cell migration. Unraveling the molecular mechanisms for the spatial and temporal regulation of Pak activity will be the next step for a better understanding of the mechanistic contribution of Paks in cellular transformation.

Materials and methods

Cell culture and microinjection

PtK1 rat-kangaroo kidney cells were cultured in Ham's F12 medium, pH 7.2 (Sigma-Aldrich), containing 25 mM Hepes (Invitrogen), 10% FBS (Gemini Bio-Products), 100 U/ml penicillin, and 0.1 mg/ml streptomycin (Invitrogen) at 37°C and 5% CO_2. U2OS osteosarcoma cells were cultured in McCoy's 5A medium (Invitrogen) containing 25 mM Hepes, 8% FBS, 100 U/ml penicillin, and 0.1 mg/ml streptomycin at 37°C and 5% CO_2. 2 d before experiments, PtK1 cells were plated on #1.5 glass coverslips (0.17 mm). Plasmids encoding GFP, GFP-tagged PID (aa 83–149 of Pak1), or an inactive mutant of the PID (GFP-PID L107F, used as a negative control) were injected into the nucleus (150 ng/µl). For adhesion strength analysis, cells were plated for 12–16 h before experiments in Ham's F12 medium containing 1% FBS on FN-coated #1.5 coverslips prepared as described in Gupton and Waterman-Storer (2006). In brief, human FN (Sigma-Aldrich) was kept at 1 mg/ml in PBS at 4°C and diluted to the appropriate concentrations (5, 10, and 30 µg/ml) for coating in PBS. Coating was performed by incubation for 2 h at 37°C. Coated surfaces were then washed three times with PBS and blocked with 1% heat-denatured BSA in PBS for 1 h at 37°C before plating the cells. Plasmids encoding GFP alone, GFP-tagged Pak1TE, or a kinase-defective mutant of Pak1 (GFP-Pak1 K299R) were injected in the cell nucleus (150 ng/µl). For FSM experiments, X-rhodamine–conjugated actin, labeled on its lysine residues, was injected into cells at 0.8–1 mg/ml. Plasmids and fluorescent actin were coinjected into the cell nucleus. For TIRF experiments, GFP-paxillin alone or in combination with myc–PID WT or myc–Pak1TE were injected into the nucleus. Protein expression was assessed by detection of the GFP from the GFP empty vector, GFP-PID (WT or L107F), GFP–Pak1TE, GFP–Pak1 K299R, or GFP-paxillin constructs. 3–6 h after injection, cells were mounted in chambers for live cell microscopy or fixed for immunofluorescence staining.

Immunofluorescence microscopy

Control and injected cells were fixed in cytoskeletal buffer (CB; 10 mM MES, 3 mM $MgCl_2$, 138 mM KCl, and 2 mM EGTA, pH 6.9) containing 4% paraformaldehyde, permeabilized in CB containing 0.5% Triton X-100, and blocked with 2% BSA in CB. Cells were then immunolabeled for the following: MHC (Sigma-Aldrich), pMLC (Ser^{19}; a gift from Y. Sasaki, Kitasato University, Tokyo, Japan), Pak1 (Cell Signaling Technology), phospho-Pak1 $Ser^{199/204}$/Pak2 $Ser^{192/197}$ (Cell Signaling Technology), paxillin (BD), and zyxin (a gift from M. Beckerle, University of Utah, Salt Lake City, UT). Appropriate Alexa Fluor 488– or 568–conjugated secondary antibodies (Invitrogen) were used at 1:500. F-actin was visualized using Alexa Fluor 350–conjugated phalloidin (Invitrogen) at 1:10. Cells were mounted on slides with ProLong Gold antifade reagent (Invitrogen) according to manufacturer's instructions. Immunofluorescence images of fixed cells were acquired on an inverted microscope (Eclipse TE 2000-U; Nikon) using a 60×/1.4 NA Plan Apo differential interference contrast objective lens (Nikon) or on a microscope (TE 2000-U; Nikon) custom modified with a TIRF illumination module as described in Adams et al. (2004) using a 100×/1.45 NA TIRF objective lens (Nikon).

Immunofluorescence analysis

Fluorescence intensity quantifications and FA measurements were performed in MetaMorph (Molecular Devices) software. All images were background subtracted before intensity measurement. Protrusion and ventral cell areas were determined by tracing the outline of the phalloidin-stained cell. The protrusion is defined by the region extending from the leading edge up to the convergence zone, which is characterized by the presence of transverse F-actin bundles. To quantify the frequency of paxillin foci length, all the detectable FAs in the protrusion of control and Pak-inhibited cells were measured. To quantify the frequency of phospho-Pak levels in FAs, paxillin immunofluorescence images were thresholded to include only FAs, and fluorescence intensity of phospho-Pak was measured in each thresholded region.

Quantification of the fluorescence of F-actin, MHC, and pMLC as a function of the distance from the cell edge was obtained with custom software written in MATLAB (MathWorks). Bands of constant distance to the cell edge were constructed, and individual fluorescence intensities were accumulated and averaged in each band to produce fluorescence intensities as a function of the distance from the cell edge.

FSM

F-actin FSM and phase-contrast time-lapse image series were acquired at 5-s intervals for 10 min using a 100×/1.4 NA Plan Apo phase objective lens (Nikon) on a spinning disk (Yokogawa; PerkinElmer) confocal microscope (TE 2000-U; Adams et al., 2003). F-actin flow rates were measured by kymograph analysis; at least five randomly placed lines normal to the free cell edge were used to construct five kymographs of each cell, and five flow rate measures were calculated for each region (lamellipodium/lamella) in each kymograph. Flow maps and F-actin polymerization/depolymerization maps were calculated by using the fsmCenter software package written in MATLAB (Danuser and Waterman-Storer, 2006).

FA dynamics

GFP-paxillin images were acquired at 15-s intervals for 30 min on a TE 2000-U microscope custom modified with a TIRF illumination module using a 100×/1.45 NA TIRF objective lens. Laser illumination was adjusted to impinge on the coverslip at an angle to yield a calculated evanescent field depth of 120 nm. Quantification of FA dynamics was performed as described in Webb et al. (2004). In brief, the fluorescent intensity of individual adhesions from cells expressing GFP-paxillin was measured over time with the use of MetaMorph software, and the background fluorescent intensity was subtracted from these values. The incorporation of paxillin into adhesions during assembly as well as the decrease in paxillin fluorescence intensity during disassembly is linear on a semilogarithmic plot of the fluorescent intensity as a function of time (Webb et al., 2004). The apparent rate constants for formation and for disassembly were determined from the slopes of these graphs. For each rate constant determination, measurements were obtained for 8–15 individual adhesions on six or seven cells.

Cell migration and leading-edge dynamics

Phase-contrast time series were acquired every 1 min for 3 h on an inverted microscope using a 20×/0.5 NA Plan Apo phase objective lens (Nikon). Cell velocity and motility parameters were calculated using MetaMorph software. Movements of individual cells were traced by tracking the translocation of the cell centroid using MetaMorph software. Leading-edge protrusive activity was determined with custom software written in MATLAB (Ponti et al., 2004) on an F-actin FSM time series captured every 5 s for 10 min.

Pak depletion

U2OS cells were transfected with 20 nM of the siRNAs (Thermo Fisher Scientific) Pak1 (D-003521-05; 5′-CAACAAAGAACAAUCACUA-3′) and Pak2 (D-003597-22; 5′-GAGCAGAGCAAACGCAGUA-3′) using Lipofectamine RNAiMAX (Invitrogen). Control siRNA oligonucleotides comprised a nontargeting siRNA pool (D-001206-13; Thermo Fisher Scientific). 72 h after transfection, cells were treated for biochemical analysis or processed for immunofluorescence microscopy.

Immunoblot analysis

Control cells, cells plated for 16 h on 5, 10, or 30 µg/ml FN, or Pak-depleted cells were lysed in ice-cold radioimmunoprecipitation assay buffer (50 mM Tris, pH 8.0, 150 mM NaCl, 1% NP-40, 0.5% sodium deoxycholate, 0.1% SDS, 1 mM EDTA, 0.2 mM PMSF, 1 µg/ml pepstatin, 2 µg/ml aprotinin, 1 µg/ml leupeptin, 1 mM sodium orthovanadate, and phosphatase inhibitor cocktail 1 [Sigma-Aldrich]). Proteins (40 µg of proteins per lane) were separated by SDS-PAGE and transferred onto nitrocellulose membrane (GE Healthcare). Membranes were probed with the primary antibodies anti-Pak1 and -Pak2 rabbit polyclonal antisera R2124 (Knaus et al., 1995), anti-pPak1 and -pPak2 rabbit polyclonal (Cell Signaling Technology), or anti-actin mouse monoclonal (C4; MP Biomedicals). Membranes were then incubated with goat anti–rabbit or anti–mouse HRP (GE Healthcare). Immunoreactive proteins were visualized using chemiluminescence (Thermo Fisher Scientific).

Online supplemental material

Fig. S1 shows levels of Pak1 and Pak2 in various cell lines and that Paks are recruited to the FAs. Fig. S2 shows the effect of Pak inhibitor–related (PIR) compound and IPA-3 treatment on Pak activity and the effects of PIR compound and IPA-3 treatment on actin dynamics. Fig. S3 shows the effects of PIR compound and IPA-3 treatment on myosin IIA and paxillin distribution. Fig. S4 shows that Pak activity regulates FA maturation. Fig. S5 shows the localization by TIRF microscopy of active Paks in cells plated

on various concentrations of FN and shows the effect of kinase-defective Pak1 on cell migration at high adhesion strength. Videos 1–4 show the effects of Pak inhibition on F-actin dynamics (Videos 1 and 2), FA turnover (Video 3), and cell motility (Video 4). Videos 5–7 show cells plated at high adhesion strength and demonstrate the effects of Pak1 expression on F-actin dynamics (Video 5), FA turnover (Video 6), and cell motility (Video 7). Online supplemental material is available at http://www.jcb.org/cgi/content/full/jcb.201010059/DC1.

This paper is dedicated to the memory of Professor Gary M. Bokoch, who has been an exceptional mentor.

We acknowledge the excellent technical assistance of B. Fowler. We thank M. Beckerle for antibodies to zyxin, Y. Sasaki for antibodies to pMLC, and K. Pestonjamasp for assistance with microscopy.

This work was supported by grants GM44428 and GM39434 (to G.M. Bokoch and C. DerMardirossian), CA117884 and DOD W81XWH-06-1-0213 (to J. Chernoff), and GM071868 (to G. Danuser). V.D. Delorme-Walker is a fellow of the American Heart Association (Western States Affiliate).

Submitted: 12 October 2010
Accepted: 31 May 2011

References

Adam, L., R. Vadlamudi, M. Mandal, J. Chernoff, and R. Kumar. 2000. Regulation of microfilament reorganization and invasiveness of breast cancer cells by kinase dead p21-activated kinase-1. *J. Biol. Chem.* 275:12041–12050. doi:10.1074/jbc.275.16.12041

Adams, M.C., W.C. Salmon, S.L. Gupton, C.S. Cohan, T. Wittmann, N. Prigozhina, and C.M. Waterman-Storer. 2003. A high-speed multispectral spinning-disk confocal microscope system for fluorescent speckle microscopy of living cells. *Methods*. 29:29–41. doi:10.1016/S1046-2023(02)00282-7

Adams, M.C., A. Matov, D. Yarar, S.L. Gupton, G. Danuser, and C.M. Waterman-Storer. 2004. Signal analysis of total internal reflection fluorescent speckle microscopy (TIR-FSM) and wide-field epi-fluorescence FSM of the actin cytoskeleton and focal adhesions in living cells. *J. Microsc.* 216:138–152. doi:10.1111/j.0022-2720.2004.01408.x

Bagheri-Yarmand, R., R.K. Vadlamudi, R.A. Wang, J. Mendelsohn, and R. Kumar. 2000. Vascular endothelial growth factor up-regulation via p21-activated kinase-1 signaling regulates heregulin-beta1-mediated angiogenesis. *J. Biol. Chem.* 275:39451–39457. doi:10.1074/jbc.M006150200

Bokoch, G.M. 2003. Biology of the p21-activated kinases. *Annu. Rev. Biochem.* 72:743–781. doi:10.1146/annurev.biochem.72.121801.161742

Brzeska, H., J. Szczepanowska, F. Matsumura, and E.D. Korn. 2004. Rac-induced increase of phosphorylation of myosin regulatory light chain in HeLa cells. *Cell Motil. Cytoskeleton*. 58:186–199. doi:10.1002/cm.20009

Cai, Y., N. Biais, G. Giannone, M. Tanase, G. Jiang, J.M. Hofman, C.H. Wiggins, P. Silberzan, A. Buguin, B. Ladoux, and M.P. Sheetz. 2006. Nonmuscle myosin IIA-dependent force inhibits cell spreading and drives F-actin flow. *Biophys. J.* 91:3907–3920. doi:10.1529/biophysj.106.084806

Carter, J.H., L.E. Douglass, J.A. Deddens, B.M. Colligan, T.R. Bhatt, J.O. Pemberton, S. Konicek, J. Hom, M. Marshall, and J.R. Graff. 2004. Pak-1 expression increases with progression of colorectal carcinomas to metastasis. *Clin. Cancer Res.* 10:3448–3456. doi:10.1158/1078-0432.CCR-03-0210

Chew, T.L., R.A. Masaracchia, Z.M. Goeckeler, and R.B. Wysolmerski. 1998. Phosphorylation of non-muscle myosin II regulatory light chain by p21-activated kinase (gamma-PAK). *J. Muscle Res. Cell Motil.* 19:839–854. doi:10.1023/A:1005417926585

Choi, C.K., M. Vicente-Manzanares, J. Zareno, L.A. Whitmore, A. Mogilner, and A.R. Horwitz. 2008. Actin and alpha-actinin orchestrate the assembly and maturation of nascent adhesions in a myosin II motor-independent manner. *Nat. Cell Biol.* 10:1039–1050. doi:10.1038/ncb1763

Cirit, M., M. Krajcovic, C.K. Choi, E.S. Welf, A.F. Horwitz, and J.M. Haugh. 2010. Stochastic model of integrin-mediated signaling and adhesion dynamics at the leading edges of migrating cells. *PLOS Comput. Biol.* 6:e1000688. doi:10.1371/journal.pcbi.1000688

Cox, E.A., S.K. Sastry, and A. Huttenlocher. 2001. Integrin-mediated adhesion regulates cell polarity and membrane protrusion through the Rho family of GTPases. *Mol. Biol. Cell*. 12:265–277.

Danuser, G., and C.M. Waterman-Storer. 2006. Quantitative fluorescent speckle microscopy of cytoskeleton dynamics. *Annu. Rev. Biophys. Biomol. Struct.* 35:361–387. doi:10.1146/annurev.biophys.35.040405.102114

Delorme, V., M. Machacek, C. DerMardirossian, K.L. Anderson, T. Wittmann, D. Hanein, C. Waterman-Storer, G. Danuser, and G.M. Bokoch. 2007. Cofilin activity downstream of Pak1 regulates cell protrusion efficiency by organizing lamellipodium and lamella actin networks. *Dev. Cell*. 13:646–662. doi:10.1016/j.devcel.2007.08.011

del Pozo, M.A., L.S. Price, N.B. Alderson, X.D. Ren, and M.A. Schwartz. 2000. Adhesion to the extracellular matrix regulates the coupling of the small GTPase Rac to its effector PAK. *EMBO J.* 19:2008–2014. doi:10.1093/emboj/19.9.2008

DiMilla, P.A., K. Barbee, and D.A. Lauffenburger. 1991. Mathematical model for the effects of adhesion and mechanics on cell migration speed. *Biophys. J.* 60:15–37. doi:10.1016/S0006-3495(91)82027-6

Dummler, B., K. Ohshiro, R. Kumar, and J. Field. 2009. Pak protein kinases and their role in cancer. *Cancer Metastasis Rev.* 28:51–63. doi:10.1007/s10555-008-9168-1

Edwards, D.C., L.C. Sanders, G.M. Bokoch, and G.N. Gill. 1999. Activation of LIM-kinase by Pak1 couples Rac/Cdc42 GTPase signalling to actin cytoskeletal dynamics. *Nat. Cell Biol.* 1:253–259. doi:10.1038/12963

Galbraith, C.G., K.M. Yamada, and M.P. Sheetz. 2002. The relationship between force and focal complex development. *J. Cell Biol.* 159:695–705. doi:10.1083/jcb.200204153

Giannone, G., B.J. Dubin-Thaler, O. Rossier, Y. Cai, O. Chaga, G. Jiang, W. Beaver, H.G. Döbereiner, Y. Freund, G. Borisy, and M.P. Sheetz. 2007. Lamellipodial actin mechanically links myosin activity with adhesion-site formation. *Cell*. 128:561–575. doi:10.1016/j.cell.2006.12.039

Goeckeler, Z.M., R.A. Masaracchia, Q. Zeng, T.L. Chew, P. Gallagher, and R.B. Wysolmerski. 2000. Phosphorylation of myosin light chain kinase by p21-activated kinase PAK2. *J. Biol. Chem.* 275:18366–18374. doi:10.1074/jbc.M001339200

Gupton, S.L., and C.M. Waterman-Storer. 2006. Spatiotemporal feedback between actomyosin and focal-adhesion systems optimizes rapid cell migration. *Cell*. 125:1361–1374. doi:10.1016/j.cell.2006.05.029

Gupton, S.L., K.L. Anderson, T.P. Kole, R.S. Fischer, A. Ponti, S.E. Hitchcock-DeGregori, G. Danuser, V.M. Fowler, D. Wirtz, D. Hanein, and C.M. Waterman-Storer. 2005. Cell migration without a lamellipodium: translation of actin dynamics into cell movement mediated by tropomyosin. *J. Cell Biol.* 168:619–631. doi:10.1083/jcb.200406063

Hsu, R.M., M.H. Tsai, Y.J. Hsieh, P.C. Lyu, and J.S. Yu. 2010. Identification of MYO18A as a novel interacting partner of the PAK2/betaPIX/GIT1 complex and its potential function in modulating epithelial cell migration. *Mol. Biol. Cell*. 21:287–301. doi:10.1091/mbc.E09-03-0232

Kiosses, W.B., R.H. Daniels, C. Otey, G.M. Bokoch, and M.A. Schwartz. 1999. A role for p21-activated kinase in endothelial cell migration. *J. Cell Biol.* 147:831–844. doi:10.1083/jcb.147.4.831

Knaus, U.G., S. Morris, H.J. Dong, J. Chernoff, and G.M. Bokoch. 1995. Regulation of human leukocyte p21-activated kinases through G protein—coupled receptors. *Science*. 269:221–223. doi:10.1126/science.7618083

Kumar, R., A.E. Gururaj, and C.J. Barnes. 2006. p21-activated kinases in cancer. *Nat. Rev. Cancer*. 6:459–471. doi:10.1038/nrc1892

Le Clainche, C., and M.F. Carlier. 2008. Regulation of actin assembly associated with protrusion and adhesion in cell migration. *Physiol. Rev.* 88:489–513. doi:10.1152/physrev.00021.2007

Machacek, M., and G. Danuser. 2006. Morphodynamic profiling of protrusion phenotypes. *Biophys. J.* 90:1439–1452. doi:10.1529/biophysj.105.070383

Manser, E., H.Y. Huang, T.H. Loo, X.Q. Chen, J.M. Dong, T. Leung, and L. Lim. 1997. Expression of constitutively active alpha-PAK reveals effects of the kinase on actin and focal complexes. *Mol. Cell. Biol.* 17:1129–1143.

Manser, E., T.H. Loo, C.G. Koh, Z.S. Zhao, X.Q. Chen, L. Tan, I. Tan, T. Leung, and L. Lim. 1998. PAK kinases are directly coupled to the PIX family of nucleotide exchange factors. *Mol. Cell.* 1:183–192. doi:10.1016/S1097-2765(00)80019-2

Nayal, A., D.J. Webb, C.M. Brown, E.M. Schaefer, M. Vicente-Manzanares, and A.R. Horwitz. 2006. Paxillin phosphorylation at Ser273 localizes a GIT1–PIX–PAK complex and regulates adhesion and protrusion dynamics. *J. Cell Biol.* 173:587–589. doi:10.1083/jcb.200509075

Ng, Y.W., D. Raghunathan, P.M. Chan, Y. Baskaran, D.J. Smith, C.H. Lee, C. Verma, and E. Manser. 2010. Why an A-loop phospho-mimetic fails to activate PAK1: understanding an inaccessible kinase state by molecular dynamics simulations. *Structure*. 18:879–890. doi:10.1016/j.str.2010.04.011

Palecek, S.P., J.C. Loftus, M.H. Ginsberg, D.A. Lauffenburger, and A.F. Horwitz. 1997. Integrin-ligand binding properties govern cell migration speed through cell-substratum adhesiveness. *Nature*. 385:537–540. doi:10.1038/385537a0

Parrini, M.C., J. Camonis, M. Matsuda, and J. de Gunzburg. 2009. Dissecting activation of the PAK1 kinase at protrusions in living cells. *J. Biol. Chem.* 284:24133–24143. doi:10.1074/jbc.M109.015271

Pollard, T.D., and G.G. Borisy. 2003. Cellular motility driven by assembly and disassembly of actin filaments. *Cell*. 112:453–465. doi:10.1016/S0092-8674(03)00120-X

Ponti, A., M. Machacek, S.L. Gupton, C.M. Waterman-Storer, and G. Danuser. 2004. Two distinct actin networks drive the protrusion of migrating cells. *Science*. 305:1782–1786. doi:10.1126/science.1100533

Ridley, A.J., M.A. Schwartz, K. Burridge, R.A. Firtel, M.H. Ginsberg, G. Borisy, J.T. Parsons, and A.R. Horwitz. 2003. Cell migration: integrating signals from front to back. *Science*. 302:1704–1709. doi:10.1126/science.1092053

Sanders, L.C., F. Matsumura, G.M. Bokoch, and P. de Lanerolle. 1999. Inhibition of myosin light chain kinase by p21-activated kinase. *Science*. 283:2083–2085. doi:10.1126/science.283.5410.2083

Sells, M.A., U.G. Knaus, S. Bagrodia, D.M. Ambrose, G.M. Bokoch, and J. Chernoff. 1997. Human p21-activated kinase (Pak1) regulates actin organization in mammalian cells. *Curr. Biol.* 7:202–210. doi:10.1016/S0960-9822(97)70091-5

Sells, M.A., J.T. Boyd, and J. Chernoff. 1999. p21-activated kinase 1 (Pak1) regulates cell motility in mammalian fibroblasts. *J. Cell Biol.* 145:837–849. doi:10.1083/jcb.145.4.837

Stofega, M.R., L.C. Sanders, E.M. Gardiner, and G.M. Bokoch. 2004. Constitutive p21-activated kinase (PAK) activation in breast cancer cells as a result of mislocalization of PAK to focal adhesions. *Mol. Biol. Cell*. 15:2965–2977. doi:10.1091/mbc.E03-08-0604

Szczepanowska, J., E.D. Korn, and H. Brzeska. 2006. Activation of myosin in HeLa cells causes redistribution of focal adhesions and F-actin from cell center to cell periphery. *Cell Motil. Cytoskeleton*. 63:356–374. doi:10.1002/cm.20125

Vicente-Manzanares, M., J. Zareno, L. Whitmore, C.K. Choi, and A.F. Horwitz. 2007. Regulation of protrusion, adhesion dynamics, and polarity by myosins IIA and IIB in migrating cells. *J. Cell Biol.* 176:573–580. doi:10.1083/jcb.200612043

Webb, D.J., K. Donais, L.A. Whitmore, S.M. Thomas, C.E. Turner, J.T. Parsons, and A.F. Horwitz. 2004. FAK-Src signalling through paxillin, ERK and MLCK regulates adhesion disassembly. *Nat. Cell Biol.* 6:154–161. doi:10.1038/ncb1094

West, K.A., H. Zhang, M.C. Brown, S.N. Nikolopoulos, M.C. Riedy, A.F. Horwitz, and C.E. Turner. 2001. The LD4 motif of paxillin regulates cell spreading and motility through an interaction with paxillin kinase linker (PKL). *J. Cell Biol.* 154:161–176. doi:10.1083/jcb.200101039

Wittmann, T., G.M. Bokoch, and C.M. Waterman-Storer. 2003. Regulation of leading edge microtubule and actin dynamics downstream of Rac1. *J. Cell Biol.* 161:845–851. doi:10.1083/jcb.200303082

Zaidel-Bar, R., C. Ballestrem, Z. Kam, and B. Geiger. 2003. Early molecular events in the assembly of matrix adhesions at the leading edge of migrating cells. *J. Cell Sci.* 116:4605–4613. doi:10.1242/jcs.00792

Zaidel-Bar, R., R. Milo, Z. Kam, and B. Geiger. 2007. A paxillin tyrosine phosphorylation switch regulates the assembly and form of cell-matrix adhesions. *J. Cell Sci.* 120:137–148. doi:10.1242/jcs.03314

Zeng, Q., D. Lagunoff, R. Masaracchia, Z. Goeckeler, G. Côté, and R. Wysolmerski. 2000. Endothelial cell retraction is induced by PAK2 monophosphorylation of myosin II. *J. Cell Sci.* 113:471–482.

Zhao, Z.S., E. Manser, T.H. Loo, and L. Lim. 2000. Coupling of PAK-interacting exchange factor PIX to GIT1 promotes focal complex disassembly. *Mol. Cell. Biol.* 20:6354–6363. doi:10.1128/MCB.20.17.6354-6363.2000